Journal of Alloys and Compounds, 213/214 (1994) 178–184
JALCOM 4049

Preparation of actinide compounds in the Oharai facility

Kenji Suzuki and Franck Wastin
Institute for Materials Research, Tohoku University, Sendai 980 (Japan)

Akira Ochiai, Tatsuo Shikama, Yoshimitsu Suzuki, Yoshinobu Shiokawa and Toshiaki Mitsugashira
The Oharai Branch, Institute for Materials Research, Tohoku University, Oharai, Ibaraki 311-13 (Japan)

Takashi Suzuki and Takemi Komatsubara
Department of Physics, Tohoku University, Sendai 980 (Japan)

Abstract

In 1990, the Oharai facility of Tohoku University began operations of its unit for research on the materials science of actinide elements. By using high vacuum zone melting and solid state electrolysis, uranium metal was refined up to a purity of 99.99 wt.%. The growth of U_2PtSi_3 and UGe_2 single crystals was achieved by the Czochralski pulling method, using a tri-arc furnace. The Bridgman method using capsulation in a tungsten metal cylinder was employed to grow UTe and USb single crystals. Thin plates of UCu_5 and UAl_2 amorphous alloys were prepared by sputter deposition. These compounds were characterized by measuring the X-ray diffraction, electrical resistivity, magnetic susceptibility and low temperature specific heat.

1. Introduction

The Oharai Branch, Institute for Materials Research, Tohoku University began the operation of its actinide experimental facility in the autumn of 1990 for common utilization by university staff and students in Japan. The main goal of the Oharai facility was originally focused on the basic research of separation chemistry in nuclear fuel cycle engineering [1]. Therefore, two steel (SS-41) cells with walls 35 cm thick and stainless steel cladding 4 cm thick have been installed in the Oharai facility for the dismantlement and chemical separation of irradiated nuclear fuels. In contrast, solid state physicists and materials scientists have been working on the purification and characterization of uranium-based intermetallic compounds in the Oharai facility, which is a unique place in Japan for university staff and students to be able to handle actinide elements.

This article reviews the purification of uranium metal, and the preparation of uranium-based crystalline intermetallic compounds, chalcogenides, pnictides and amorphous alloys which have been performed so far at the Oharai facility.

2. Purification of uranium metal

The purification of commercially supplied uranium metal of a purity higher than 99 wt.% was carried out using a combination of r.f. zone melting and d.c. electrotransport [2]. Since uranium metal is chemically very active and has a strong affinity for interstitial gas elements, such as hydrogen, nitrogen, oxygen, etc., the purification had to be carried out in a suitable environment to prevent the uranium metal from sorbing impurity elements into it.

We used a water-cooled copper crucible to keep the melt of the uranium metal in high vacuum and helium atmospheres during the r.f. zone melting process, because uranium metal is incompatible with almost all refractory metals above its melting temperature. A floating zone melting technique was avoided in this work, since self-sustaining the melt of uranium metal is not easy. Therefore, r.f. heating was chosen in our zone melting work. Electron beam heating was not used in the zone melting furnace, because tungsten vapor coming from the filament often contaminates a melted sample. The r.f. zone melting furnace used in this work is shown schematically in Fig. 1.

The operating conditions of the r.f. zone melting furnace are summarized in Table 1. A uranium metal rod 10 mm in diameter and 150 mm long was zone melted in the copper crucible with a zone width of 15 mm at a scanning rate of 1.5 mm min^{-1} in a high vacuum. The zone melting process was repeated several times in the high vacuum, followed by zone melting

SSDI 0925-8388(94)04049-A

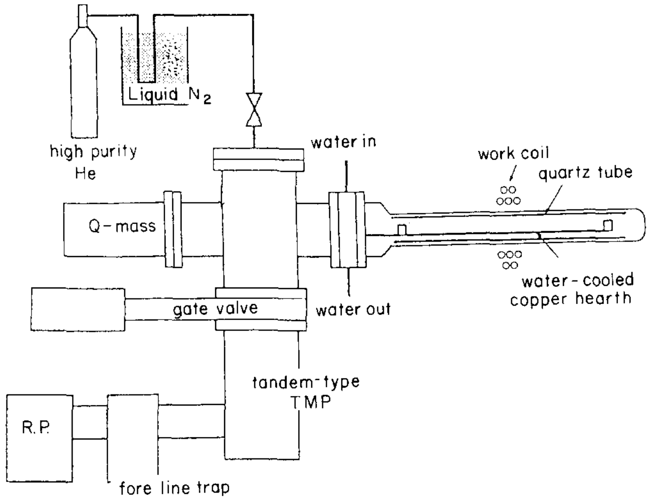

Fig. 1. R.f. zone melting furnace used for refining uranium metal.

under helium gas at a pressure of 1 atm. The introduction of helium gas into the furnace drastically reduces the irregular vibration of the melt of uranium metal during the process of zone melting.

After cutting off one-third from the end of the refined uranium metal rod, the process of zone melting in a high vacuum and under helium gas was continued several times. As shown in Table 2, almost all the metallic impurities are removed (except for calcium) by the zone melting. The net purity of the uranium metal refined by the zone melting is estimated to be higher than 99.99 wt.%.

Since hydrogen, nitrogen and oxygen cannot be removed by the zone melting, we applied solid state electrolysis, using the d.c. electrotransport technique, to the uranium metal rod refined by the zone melting. A schematic illustration of the furnace used for this solid state electrolysis is shown in Fig. 2. The operating conditions of the furnace are listed in Table 1. However, we have not yet confirmed the quantities of these impurities which are removed from the uranium metal by the solid state electrolysis.

Since the refined uranium metal rod was often left in ambient atmosphere, which resulted in the uptake of interstitial gas impurities, such as hydrogen and oxygen, we observed a low residual resistivity ratio (r.r.r.), as shown in Fig. 3. Although the absolute value of the r.r.r. is sensitive to the content of gas element impurities, it is interesting to note that the behavior of the r.r.r. in Fig. 3 represents well the concentration profile of metallic impurities in the uranium metal refined by the zone melting.

3. Growth of single crystals of uranium-based compounds by the Czochralski pulling method

By using the refined uranium metal mentioned in Section 2, ternary U–Pt–Si [3] and the binary U–X (X≡Ge, Ru, Rh, Ir) [4] compounds were prepared. In particular, U_2PtSi_3 and UGe_2 were grown into single crystals by means of the Czochralski pulling method, using a tri-arc furnace.

Figure 4 shows a schematic diagram of the tri-arc furnace used in this work [5]. A water-cooled copper crucible holding the melt of the materials is rotated, as is a crystalline seed. During the operation, we could watch through a water-cooled double glass wall the melting and pulling of the sample.

In the U–Pt–Si ternary system, the two compounds $UPtSi_2$ and U_2PtSi_3 were synthesized in this work. However, we failed to grow a single crystal of $UPtSi_2$, because of its incongruent melting. Polycrystalline $UPtSi_2$ is a ferromagnetic compound with Curie temperature $T_c = 86$ K, and has an effective Bohr magneton number of $2.3\mu_B$ in the paramagnetic state.

The temperature dependence of the inverse magnetic susceptibility of the U_2PtSi_3 single crystals is shown in Fig. 5 for the two different directions of magnetic field applied to the crystalline axes. In both directions, the Curie–Weiss law is followed, with an effective Bohr magneton number of $2.1\mu_B$ at high temperatures. At low temperatures, we observed magnetic remanence; it disappeared around 8 K, which corresponds to the Curie temperature. Below the Curie temperature, the magnetization gradually increased with magnetic field,

TABLE 1. Operating conditions of r.f. zone melting furnace and solid state electrolysis furnace [2]

	Solid state electrolysis	R.f. zone melting	
Vacuum system	Ion pump, Titanium sublimation pump with liquid N_2 shroud,	Vacuum system	Tandem-type turbomelecular pump
	Turbomolecular pump	Base pressure	$\approx 7\times10^{-9}$ Pa
Base pressure	$\approx 4\times10^{-9}$ Pa	Output power	15 kW
Current	d.c. 0–1000 A	Frequency	400 kHz
Voltage	d.c. 0–6 V	Sample length	200 mm max.
Sample length	120 mm max.	Width of molten zone	≈ 15 mm

TABLE 2. Metallic impurity contents in uranium metal rod refined by zone melting [2]

Position	Element (wt.ppm)										
	Al	Ca	Cr	Cu	Fe	Mn	Ni	Pb	Si	Sn	Zn
a	10	9.1	1.0	3.6	14.4	–	9.2	0.2	21.5	0	0.4
b	10	3.5	2.3	6.7	53.8	0	32.9	–	28.9	1.2	0.4
c	10	4.6	4.2	11.1	188.4	0.2	96.8	0.2	66.7	6.5	0.8
1	8	8.6	0.9	2.2	8.6	–	5.5	–	17.8	0.9	0.2
2	13	6.6	2.0	4.3	47.8	0	28.5	–	26.5	1.8	0.7
3	25	11.2	4.2	7.1	146.2	0	80.3	0.6	70.0	4.6	1.0
Before refining	13	4.4	2.3	17.1	53.1	6.9	33.8	9.6	34.3	2.0	2.2

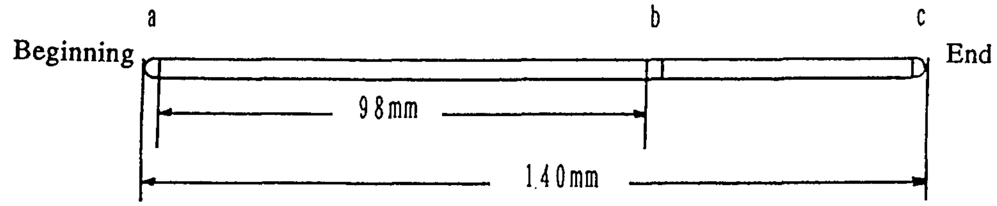

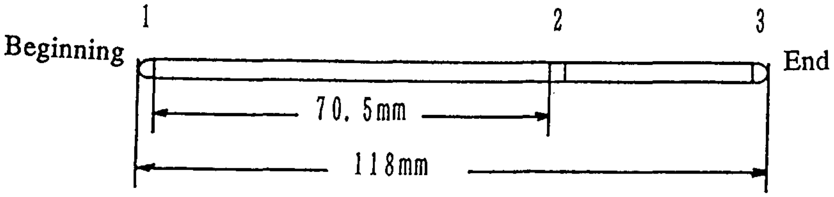

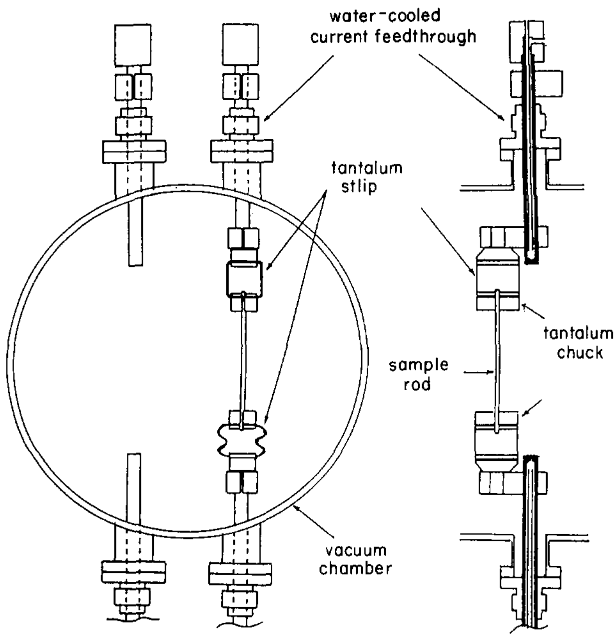

Fig. 2. D.c. electrotransport furnace used for solid state electrolysis of uranium metal.

but did not saturate up to a magnetic field of 90 kOe. The magnetic moments at 90 kOe were $0.88\mu_B$ for $H \parallel a$ axis and $0.50\mu_B$ for $H \parallel c$ axis, which are smaller than the values of $3.20\mu_B$ for the $(5f)^2$ or $3.27\mu_B$ for the $(5f)^3$ free-ion state.

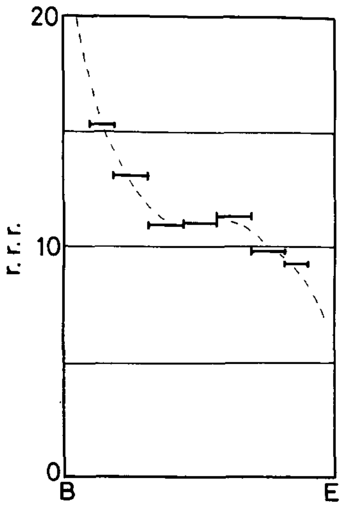

Fig. 3. Residual resistivity ratio of uranium metal rod refined by zone melting, where B is the beginning of the uranium metal rod and E is the end of it.

A plot of C/T vs. T^2 for the specific heat of U_2PtSi_3 single crystals, which provides a direct way to examine the heavy fermion behavior of the compound, is also shown in Fig. 5. No anomalies are found at the Curie temperature. The extrapolation of C/T to 0 K provides a value of $\gamma(0) = 200$ mJ K^{-2} (mol U)$^{-1}$, which is a medium weight magnitude for heavy fermion materials.

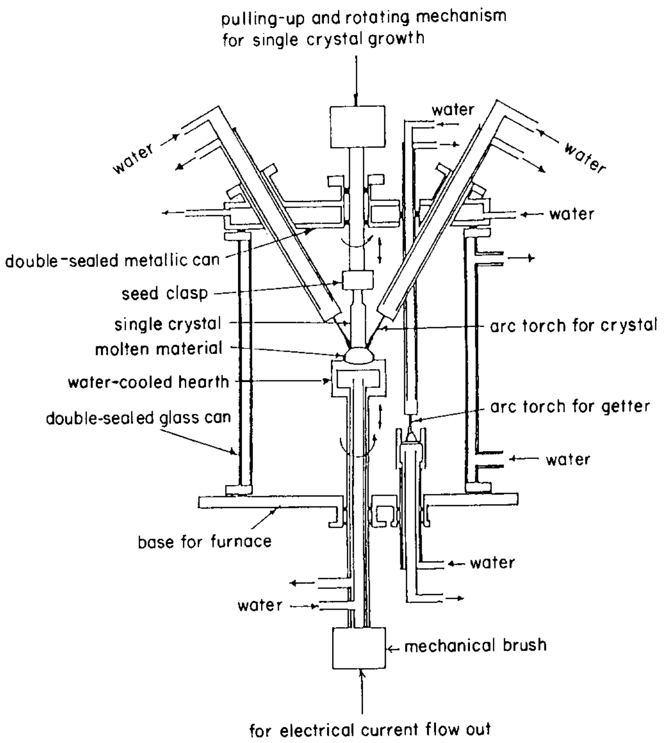

Fig. 4. Tri-arc furnace used to grow single crystals of uranium-based intermetallic compounds.

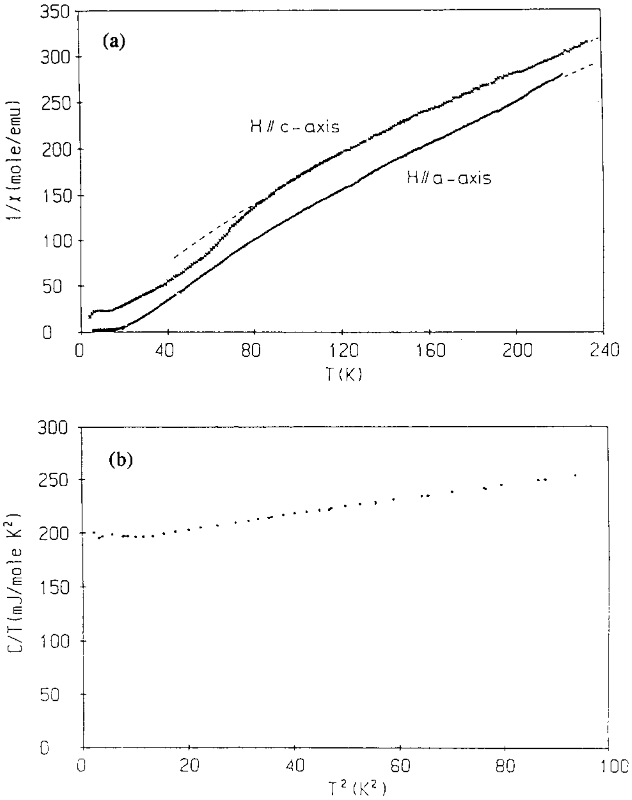

Fig. 5. (a) Temperature dependence of inverse magnetic susceptibility ($1/\chi$) of U_2PtSi_3 single crystal [3] and (b) that of low temperature specific heat of U_2PtSi_3 single crystal [3].

Four different compounds – U_7Ge, U_5Ge_3, U_3Ge_4 and UGe_2 – which exist in the U–Ge binary system were prepared using the tri-arc furnace. Their properties are shown in Table 3. A large, high quality, single crystal of UGe_2 3–4 mm in diameter and 40 mm long was grown by the Czochralski pulling method, using the tri-arc furnace. The residual resistivity at 0.5 K and the r.r.r. were 0.1 $\mu\Omega$ cm and 740, respectively, for this material. The de Hass–van Alphen effect was successfully observed to provide a large cyclotron carrier mass of 2.3–25m_0. The 5f electrons in UGe_2 are essentially itinerant and are strongly correlated, similarly to UPt_3.

4. Preparation of single crystals of uranium chalcogenides and pnictides by the Bridgman method

U–chalcogen and U–pnictogen systems often form very stable compounds that have high melting temperatures. Since the chalcogens and pnictogens are volatile, melting these compounds in a closed vessel is preferred. In this work, we capsulated powders of prereacted uranium and tellurium (or antimony) into a tungsten cylinder by electron beam welding, and melted them by r.f. heating the tungsten cylinder [6]. Single crystals of UTe and USb were grown by the Bridgman method [7].

The specific heats of UTe and USb were measured over a wide temperature range of 2–300 K, as shown in Fig. 6. A λ-type sharp peak profile was observed on both curves. The peak appearing at 102 K for UTe corresponds to ferromagnetic ordering, while the peak at 218 K corresponds to the antiferromagnetic ordering of USb. The specific heat contributed from phonons is limited to $3Nk_B = 50$ J mol^{-1} K^{-1} at high temperatures. Figure 6 shows that a large portion of the specific heat is contributed by the magnetic term, especially for USb, which has a long peak tailing off as room temperature is approached.

The electrical resistivity of an as-grown single crystal of USb (NaCl-type structure) has a high value (600 $\mu\Omega$ cm) at room temperature; with decreasing temperature, it gradually increases until 240 K. Below 240 K, the resistivity rises drastically and reaches a maximum at around 150 K, which is followed by a steep decrease to the residual resistivity of about 40 $\mu\Omega$ cm. With annealing, both the maximum and residual resistivities decrease. It should be noted that a very large positive magnetoresistance is observed for the USb single crystal annealed at 1373 K, as shown in Fig. 7. Furthermore, the carrier number in the USb single crystal annealed at 1373 K is estimated to be only 1.8% of the uranium atom number below 4.2 K, based on the measurement of a Hall coefficient value of -0.2 cm^3 C^{-1}.

TABLE 3. Characterization of U_7Ge, U_5Ge_3, U_3Ge_4 and UGe_2, where T_0 is the superconducting transition temperature and T_c is the Curie temperature [4]

Substance	Crystal structure	Characteristic temperature	Specific heat coefficient (mJ K^{-2} (mol U)$^{-1}$
U_7Ge		Superconductive $T_0=1.40$ K	16
U_5Ge_3	Hexagonal	Superconductive $T_0=0.99$ K	36
U_3Ge_4	Orthorhombic	Ferromagnetic $T_c=94$ K	
UGe_2	Orthorhombic	Ferromagnetic $T_c=52$ K $\mu_{sat}=1.4\mu_B$ (*c* axis)	35

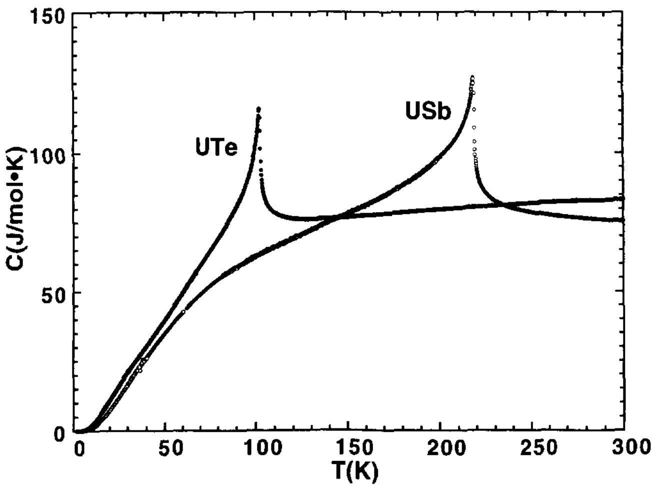

Fig. 6. Variation of specific heat of UTe and USb single crystals with temperature [7].

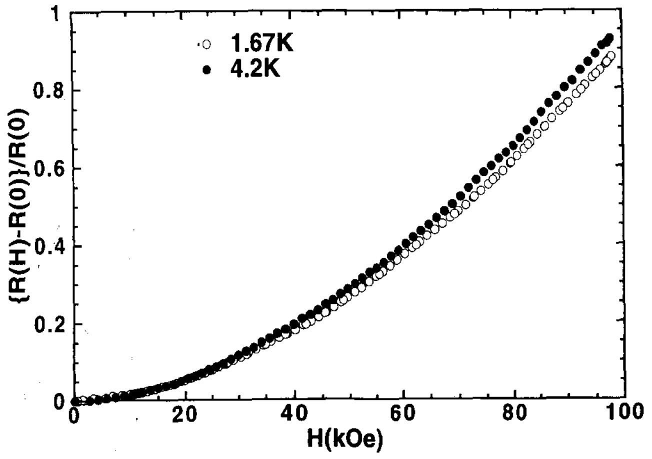

Fig. 7. Variation of magnetoresistance of USb single crystals at 1.67 K (○) and 4.2 K (●).

The electrical resistivity of the UTe (NaCl-type structure) single crystals is about 300 μΩ cm at room temperature; it gradually increases to reach a broad maximum at around 150 K, followed by a sharp drop to the residual resistivity of about 130 μΩ cm.

As starting materials for growing single crystals of uranium chalcogenides and pnictides, we prepared various polycrystalline compounds, such as US, US_2, USe, U_3Se_4, USe_2, UP, U_3P_4, UP_2, UAs, U_3As_4, UAs_2, etc., by r.f. melting of the materials in tungsten or molybdenum metal cylinders [8].

5. Formation of uranium-based amorphous alloys by r.f. sputter deposition

UCu_5 and UAl_2 amorphous alloys were prepared by r.f. argon plasma sputter deposition. The sputter deposition apparatus used in this work is illustrated in Fig. 8. The goal for designing this apparatus is to form a thin plate (several hundred micrometers in thickness) of uranium-based amorphous alloys, by using a small area alloy target (25 mm in diameter), and achieve this within a reasonable deposition duration. Therefore, an r.f. magnetron system was employed to confine an argon plasma into a narrow space between the alloy target and substrate. After evacuating the sputtering chamber down to 3×10^{-7} Torr and presputtering, sputtering was carried out for 2 –3 days under 5×10^{-3} Torr of argon gas. So far, we have successfully obtained thin plates (0.1–0.5 mm thick and 20 mm×10 mm in area) of UCu_5 and UAl_2 amorphous alloys.

Figure 9 shows the X-ray diffraction pattern of a UCu_5 thin plate obtained by sputter deposition, which is a typical profile for our amorphous alloys. The specific heat of the UCu_5 amorphous alloy shows a drastic increase in the C/T *vs.* T^2 plot below 3 K, as shown in Fig. 10. The electrical resistivity has a broad maximum at around 250 K, but it monotonically increases with further decreasing of the temperature. The magnetic susceptibility obeys the Curie–Weiss law at high temperatures and also shows a tiny step at 240 K. These results are summarized in Figs. 11 and 12.

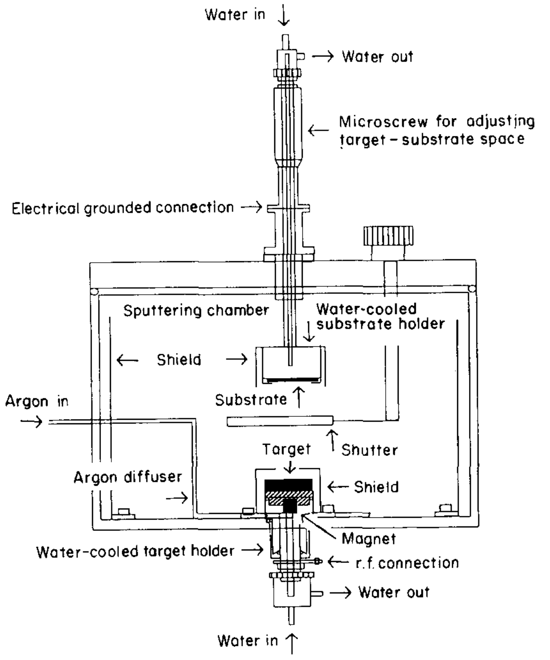

Fig. 8. R.f. sputter deposition apparatus used to prepare thin plate of UCu_5 amorphous alloy.

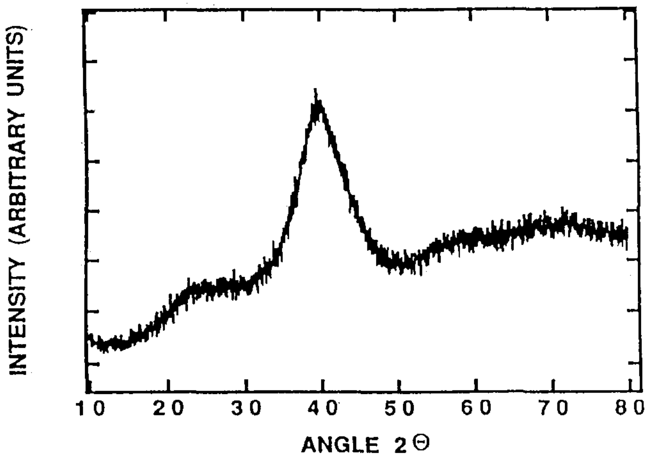

Fig. 9. X-ray diffraction pattern of UCu_5 amorphous alloy.

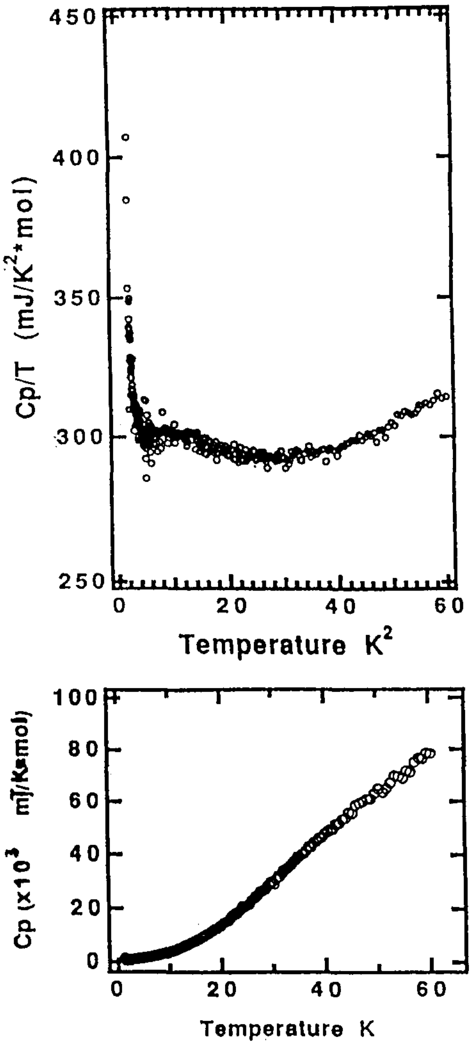

Fig. 10. Low temperature specific heat of UCu_5 amorphous alloy.

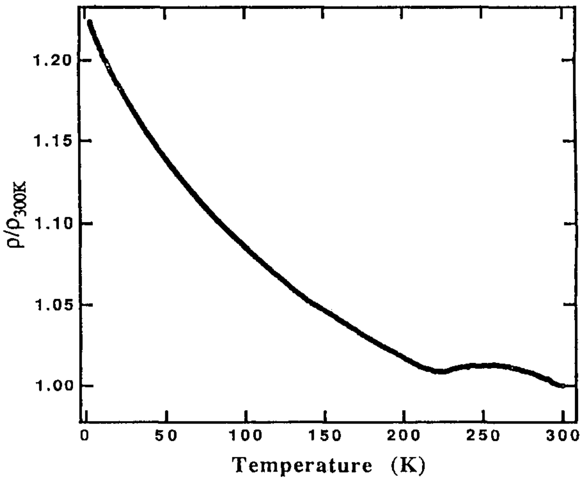

Fig. 11. Temperature dependence of electrical resistivity ρ of UCu_5 amorphous alloy.

In contrast to crystalline UCu_5, which orders antiferromagnetically at $T_N = 15$ K [9], amorphous UCu_5 obviously suppresses the magnetic ordering temperature below 4.2 K. However, a great enhancement of the low temperature specific heat still occurs in amorphous UCu_5. Such behavior has been observed also for amorphous $CeCu_6$ [10].

6. Concluding remarks

In the Oharai facility, both the separation chemistry of spent nuclear fuels and the solid state physics of actinide compounds are pursued. In particular, the

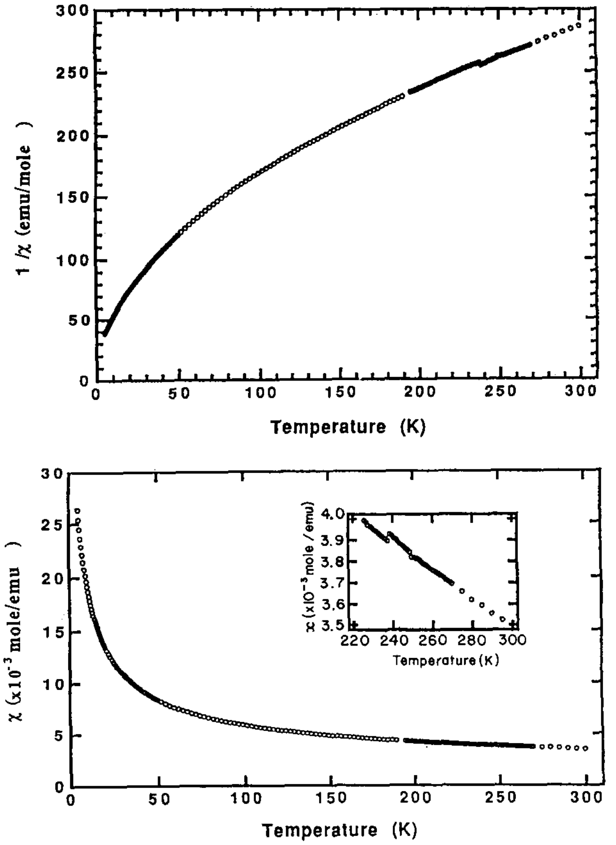

Fig. 12. Variation of magnetic susceptibility of UCu_5 amorphous alloy with temperature.

materials science-oriented development in actinide-based compounds and alloys is emphasized. In developing opto-magnetic memory media and hard magnet materials, the formation of U-transition metal-based multicomponent amorphous alloy films has been initiated. The preparation and purification of neptunium metal are expected to be an important project supporting the solid state physics of actinides in the Oharai facility.

Acknowledgments

The work described in this paper was supported by Grant-in-Aid for Scientific Research on Priority Areas 1988–1991 “Studies of the Solid State Properties of Actinide Compounds”; by the Ministry of Education, Science and Culture in Japan; by the NEDO International Joint Research Grant, 1989–1991 “Electrical Properties and Fundamental Characteristics of Heavy Fermion”; and by the New Energy and Industrial Technology Development Organization in Japan.

References

1 T. Mitsugashira, *Proc. Symp. on Advanced Nuclear Engineering, Inst. Mater. Res., Tohoku University, Sendai,* March 1988, p. 137 (in Japanese).

2 K. Suzuki, T. Shikama and A. Ochiai, Purification of uranium metal, *Physical Properties of Actinide and Rare Earth Compounds — Search for Heavy Fermion Characters, JJAP Ser., 8* (1993) 15.

3 T. Komatsubara, N. Sato, M. Kagawa and K. Tanaka, Research and characterization of new uranium-based ternary compounds, in *Physical Properties of Actinide and Rare Earth Compounds — Search for Heavy Fermion Characters, JJAP Ser., 8* (1993) 20.

4 Y. Onuki, S.W. Yun, I. Umehara, K. Satoh, H. Sato, S. Takayanagi, T. Komatsubara, M. Shikama and A. Ochiai, Magnetic and electrical properties of U–Ge and U–X (X = Ru, Rh, Ir) intermetallic compounds, *Physical Properties of Actinide and Rare Earth Compounds — Search for Heavy Fermion Characters, JJAP Ser., 8* (1993) 24.

5 A.A. Menovsky and J.J.M. Franse, *J. Cryst. Growth, 65* (1983) 286.

6 T. Suzuki, Single crystal preparation and characterization of f electron's chalcogenides and pnictides — Part I, Facilities for rare earth compounds in Department of Physics, Tohoku University, *Physical Properties of Actinide and Rare Earth Compounds — Search for Heavy Fermion Characters, JJAP Ser., 8* (1993) 44.

7 A. Ochiai, Y. Suzuki, T. Shikama, K. Suzuki, E. Hotta, Y. Haga and T. Suzuki, submitted for publication in *J. Alloys Comp.*

8 T. Suzuki, H. Shida, A. Ochiai, M. Shikama and K. Suzuki, Single crystal preparation and characterization of f electron's chalcogenides and pnictides — Part II, Facilities for the preparation of chalcogenides and pnictides of actinides in Oarai Branch of IMR, Tohoku University, *Physical Properties of Actinide and Rare Earth Compounds — Search for Heavy Fermion Characters, JJAP Ser., 8* (1993) 55.

9 H.R. Ott, H. Rudigier, E. Felder, Z. Fisk and B. Batlogg, *Phys. Rev. Lett., 55* (1985) 1595.

10 K. Sumiyama, H. Amano, H. Yamauchi, K. Suzuki and T. Suzuki, *J. Phys. Soc. Jpn., 61* (1992) 2359.